Solid State Communications 188 (2014) 23–26

Contents lists available at ScienceDirect

Solid State Communications

journal homepage: www.elsevier.com/locate/ssc

Exchange bias in room-temperature epitaxial Fe_3O_4 film

Xiangbo Liu, Huibin Lu*, Meng He, Kuijuan Jin, Guozhen Yang

Beijing National Laboratory for Condensed Matter Physics, Institute of Physics, Chinese Academy of Sciences, Beijing 100190, People's Republic of China

ARTICLE INFO

Article history:
Received 23 November 2013
Received in revised form
25 February 2014
Accepted 1 March 2014
By F. Peeters
Available online 6 March 2014

Keywords:
A. Fe_3O_4
C. Antiphase domain boundary
D. Exchange bias
D. Training effect

ABSTRACT

We have grown 100-nm-thick epitaxial Fe_3O_4(111) film on α-Al_2O_3(0001) substrate at room temperature by the laser molecule beam epitaxy method. Exchange bias effect is observed once the film is cooled from 300 K to 5 K in the presence of a magnetic field, characterized by the shift and expansion of magnetic hysteresis loops. The observed exchange bias effect is related to the exchange coupling between antiferromagnetic Fe–O–Fe superexchange interactions at antiphase domain boundaries and ferromagnetic spins in the neighboring Fe_3O_4 domains. The magnitudes of the exchange bias field and coercive field show strong dependence on magnetic and thermal histories.

1. Introduction

Since the pioneering work on the exchange bias (EB) effect by Meiklejohn and Bean in 1956, when they studied the magnetic properties of Co/CoO particles [1], EB effect has been becoming a very important topic in the field of magnetism. EB effect is an interfacial magnetic phenomenon characterized by the shift and broadening of magnetic hysteresis loop and is often observed in a system with a ferromagnetic/antiferromagnetic (FM/AFM) interface. Over the past six decades, a great number of efforts have been spent on the theoretical and experimental researches about the EB phenomenon. To date, a complete model of EB effect still remains to be developed, but it has not influenced the progress of experimental work at all. EB phenomenon is widely observed in various multicomponent systems which have well-defined FM/AFM interfaces, such as core–shell nanostructures, bi- or multilayer films, and inhomogeneous alloys [2]. Some hard/soft FM heterostructures also present EB effect [3]. In addition, phase separation systems can show EB phenomena too, such as $La_{1-x}Sr_xCoO_3$, Sr_2YbRuO_6, and $La_{1-x}Pr_xCrO_3$ [4–6].

Fe_3O_4 is a famous half-metal ferrimagnetic with a high Curie temperature (T_C) of 860 K and high spin polarization of nearly 100%. Fe_3O_4 crystallizes in cubic inverse spinel structure with a lattice constant of $a=0.839$ nm. Epitaxial Fe_3O_4 films can be grown on $MgAl_2O_4$, $SrTiO_3$, MgO and α-Al_2O_3 substrates easily [7–10]. Due to these advantages, Fe_3O_4 films always play the role of FM layer in spintronics devices [11]. It is reported that epitaxial Fe_3O_4 films contain a kind of natural growth defect—antiphase domain boundaries (APBs) which have not been observed in bulk Fe_3O_4. At the APBs, the oxygen sublattices are continuous, whereas the cation chains are disrupted. The superexchange interactions occurring across the APBs can be either FM or AFM depending on the configuration of APBs [12], which are more complicated than that in the Fe_3O_4 domains. The presence of APBs produces a great influence on the electric and magnetic properties of Fe_3O_4 films. Recently, we observed that Fe_3O_4(111) films can be grown layer-by-layer on *c*-plane sapphire when the substrates were kept at room temperature [13]. EB effect has been observed in these films, and the EB field (defined as $H_E=|H_{C+}+H_{C-}|/2$, H_{C+} and H_{C-} are coercivity field in the positive and negative direction, respectively) increases with increasing density of APBs. In the present work, the EB effect was studied in a room-temperature epitaxial 100-nm-thick Fe_3O_4 film in detail, which shows strong dependence on magnetic and thermal history.

2. Experimental

A 100-nm-thick room-temperature epitaxial Fe_3O_4 film was grown on annealed α-Al_2O_3(0001) substrate by laser molecular beam epitaxy (Laser-MBE). A high-purity iron ingot ($>99.99\%$) was used as the target. The target-to-substrate distance was fixed at 70 mm. The beam of a XeCl excimer laser (308 nm, 20 ns, and 2 Hz) was focused on the iron target with an energy density of about 1.5 J/cm^2. The base pressure of the epitaxy chamber was 1×10^{-5} Pa. During the entire preparation process, the substrates were kept at room temperature ($\sim$300 K), and oxygen pressure was maintained

* Corresponding author.
E-mail address: hblu@iphy.ac.cn (H. Lu).

http://dx.doi.org/10.1016/j.ssc.2014.03.002
0038-1098

at 1×10^{-3} Pa. The film thickness was monitored by real-time reflection high energy electron diffraction (RHEED). The crystal structure was characterized by X-ray diffraction (XRD) using a Cu Kα radiation. Magnetic hysteresis loops were measured using a vibrating sample magnetometry (VSM) (PPMS-9T, Quantum Design).

3. Results and discussion

An XRD $\theta-2\theta$ scanning curve of as-prepared $Fe_3O_4(111)$ film on α-$Al_2O_3(0001)$ substrate is plotted in Fig. 1. Besides the diffraction signals from the substrate, only a series of peaks ascribed to $Fe_3O_4(hhh)$ planes have been detected, without any trace of other impurity phases or random planes. This indicates that the room temperature epitaxial Fe_3O_4 thin film crystallizes in single phase and grows along the [111] direction.

The in-plane zero-field-cooled (ZFC) and field-cooled (FC) magnetic hysteresis (M–H) curves for the Fe_3O_4 film were measured at 5 K. The measurement procedure was performed as follows: firstly, the sample was cooled from room temperature to 5 K without external field, and then a M–H loop in the field range of -30 to $+30$ kOe was recorded, that is the ZFC M–H; secondly, the sample was heated up to 300 K, and then a $+5$ kOe field was applied in the parallel direction of the film plane, the FC M–H curve was recorded after the temperature decreased to 5 K; thirdly, we repeated the FC M–H measurement, but the cooled field was set at -5 kOe field.

As shown in Fig. 2, the ZFC M–H curve is symmetric about the original point, but the FC M–H curves display apparent asymmetry. In comparison with the ZFC M–H curve, when the film is cooled in the presence of a positive field, the center of the FC ($+5$ kOe) M–H curve shifts in the negative field direction by approximately 760 Oe, which is the magnitude of H_E; when the film is cooled in a negative field, the loop shifts in the positive field direction by $H_E=580$ Oe. This is a typical feature of EB effect. Another typical feature of EB phenomenon—the increased coercive field (H_C) is also observed clearly in here. In Fig. 2, we can see the values of H_C, defined as $H_C=(H_{C+}-H_{C-})/2$, are 1270, 1728, and 1574 Oe for ZFC M–H, FC ($+5$ kOe) M–H, and FC (-5 kOe) M–H, respectively. Therefore, we can conclude that EB effect is observed in the room-temperature epitaxial Fe_3O_4 film.

In general, EB phenomenon originates from the exchange couplings happening across the FM/AFM interfaces. Herein, the presence of EB in a homogeneous epitaxial film is atypical for the lack of a clear boundary between FM and AFM spins. A fact should

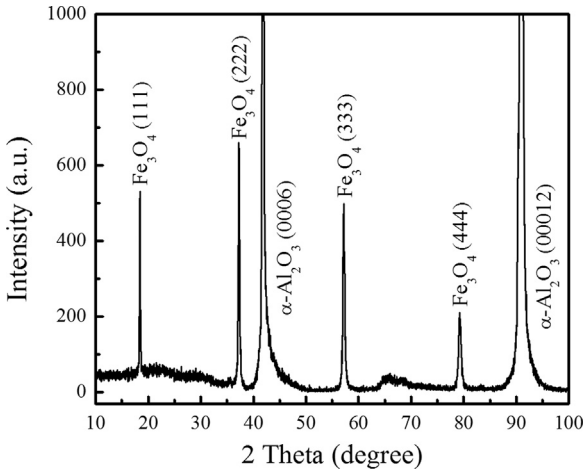

Fig. 1. A typical XRD $\theta-2\theta$ scanning profile for the 100-nm-thick room-temperature epitaxial $Fe_3O_4(111)$ film on α-$Al_2O_3(0001)$ substrate.

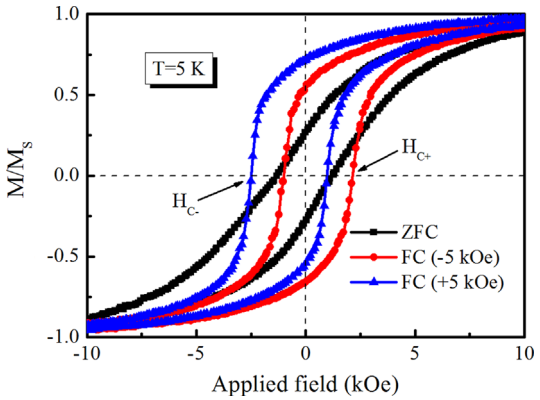

Fig. 2. (Color online) Zero-field-cooled (ZFC) and field-cooled (FC) ($H=\pm5$ kOe) magnetic hysteresis loops of Fe_3O_4 film measured at 5 K.

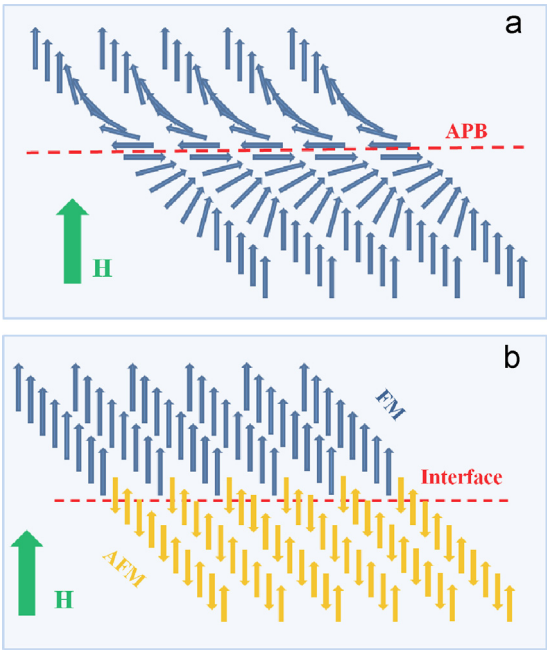

Fig. 3. (Color online) (a) A schematic of spin structure at the APBs with AFM coupling in saturation field, and (b) a schematic of spin structure in a common FM/AFM system.

be noted that a large fraction of 180° Fe–O–Fe superexchange interactions across APBs is AFM in nature [14]. In fact, the distribution, size and shape of antiphase domains are random, so the superexchange interactions at APBs are very complicated [12]. A schematic of spin arrangement near the AFM APB in a sufficient field is shown in Fig. 3(a). The spins in Fe_3O_4 domain areas align along the external field (H), while the spins close to the APBs gradually rotate toward 90° out of plane with respect to H to facilitate AFM couplings across the boundary [15,16]. The directions of the antiparallel spins are pinned by the domain walls. Similar to the AFM layer in a common FM/AFM system (as shown in Fig. 3(b)), these AFM exchange interactions exert a pinning action to the neighboring spins in FM domains. We can see that the pinning direction of AFM spins at APBs is different from that in FM/AFM system. When H is reversed, the FM spins far from the APBs rotate with the external field, but the AFM spins at APBs keep unchanged due to the strong anisotropy. The AFM spins impose an additional microscopic torque on the neighboring FM spins to keep them in their original direction. As a result, a larger H is needed to reverse the FM spins completely. On the contrary, when

H rotates back to its original direction, a smaller H can turn back the FM spins totally. This process reflected in the experimental results is the shift of M–H loop and the increase of coercive field, in comparison with the intrinsic values of Fe_3O_4, just as the results of Fig. 2.

One of the interesting characteristics of EB is that the EB field shows a very strong dependence on the magnetic history. The consecutive M–H measurements after field cooling show that the magnitude of H_E decreases with ordinal measurement cycles, known as the training effect. To study the training effect of Fe_3O_4 film, 10 full M–H measurement cycles have been carried out after the sample was cooled from 300 to 5 K within a field of 5 kOe. The 10 FC M–H loops around the low field region (−4 to+4 kOe) are shown in Fig. 4(a). Most importantly, both the coercivity (H_C) and exchange bias field (H_E) decrease obviously with the measurement cycles. Namely, the training effect is observed in the room-temperature epitaxial Fe_3O_4 film indeed. Fig. 4(b) shows the value of H_C as a function of measurement cycles (n). The up-triangles and down-triangles in the insets of Fig. 4(b) are $-H_{C-}$ and H_{C+}, respectively. It is very clear that H_C decreases monotonously with the cycle number as expected. The first FC M–H loop shows H_C=1680 Oe, whereas it decreases to 1060 Oe for n=10. With respect to H_E, it decreases quickly from $H_E(1)$=780 Oe to $H_E(6)$=425 Oe. Subsequently, it transits into a moderate way, H_E is 415 Oe after 10 cycles. Generally, the variation of H_E can be described by a phenomenological relation [17]:

$$H_E(n)-H_E(\infty) \propto 1/n^{1/2} \quad (1)$$

where n is the number of measurement cycles, $H_E(n)$ and $H_E(\infty)$ are the EB fields of n and infinite cycles, respectively. $H_E(\infty)$ can be obtained by extrapolating $H_E(n)$ value to $n=\infty$ in Fig. 4(c). The spots in the inset of Fig. 4(c) are the values of $H_E(n)-H_E(\infty)$, and the solid lines are fitted results using formula (1). It is found that the EB field obeys the power-law (1) approximately. When the measurement cycle $n>6$, it deviates from this relation, which may indicate that the magnetic property of this system tends to be steady after the repeated measurements.

After the magnetic training, the temperature-dependence of the EB effect was measured in the range of 5–170 K. The temperature-dependent H_E and H_C are plotted in Fig. 5. The values of H_E and H_C are derived from the FC M–H loops at each temperature. The magnitude of H_E decreases as temperature increased. H_E is 415 Oe at 5 K. After heating the sample up to 100 K, H_E reduces to 35 Oe. And the magnitude of H_E is only 10 Oe at 170 K. The variation of coercivity is slightly complicated; a turning point is observed in the H_C–T curve. The value of H_C is 1060 Oe at 5 K, but it increases to 1295 Oe when the temperature rises to 30 K. Subsequently, H_C decreases with the elevating temperature monotonously. It should be noted that the value of H_C (5 K) is obtained after 10 measurement cycles, but it is 1680 Oe at the first measurement cycle. Therefore, H_C should decrease with increasing temperature monotonously. It seems that the training effect at low temperature cannot influence the coercivity at higher temperature.

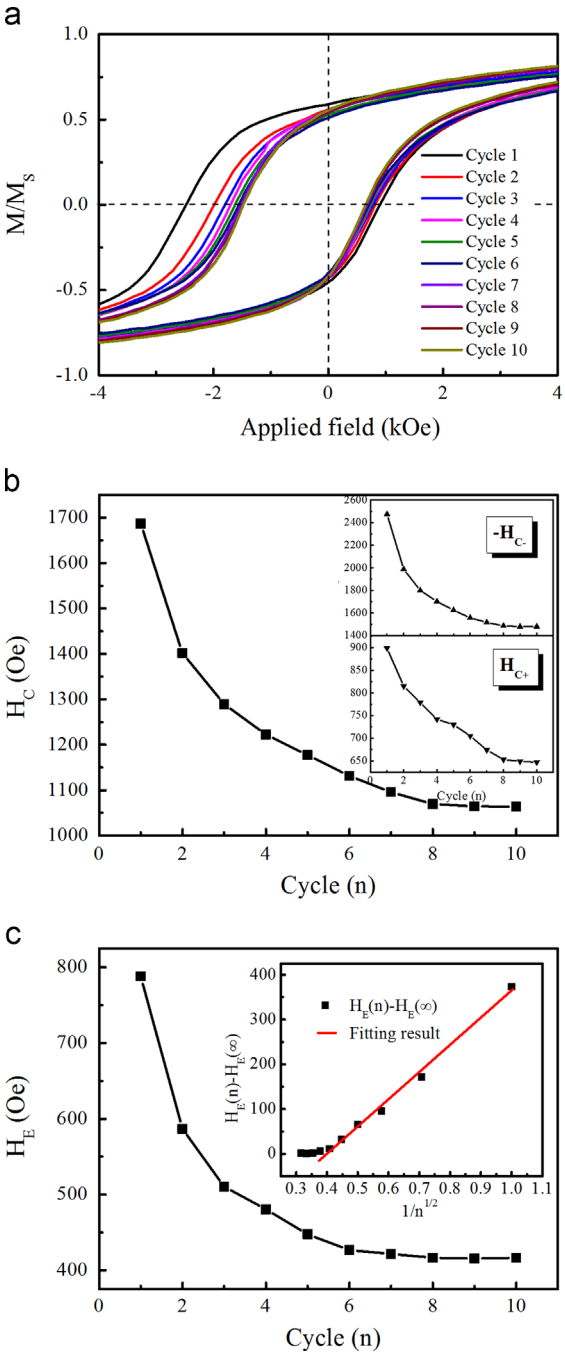

Fig. 4. (Color online) Training effect of Fe_3O_4 film at 5 K. (a) Ten consecutively measured M–H curves around the low-field region (from −4 kOe to +4 kOe), (b) the values of H_C versus the number of measurement cycles, the insets show the cycle-dependence of the coercive fields H_{C-} (up triangles) and H_{C+} (down triangles), and (c) the cycle-dependence of exchange bias H_E, the inset is the fitted result of H_E by power-law (1).

4. Conclusions

In summary, a 100-nm-thick Fe_3O_4(111) film has been epitaxially grown on α-Al_2O_3(0001) substrate at room temperature.

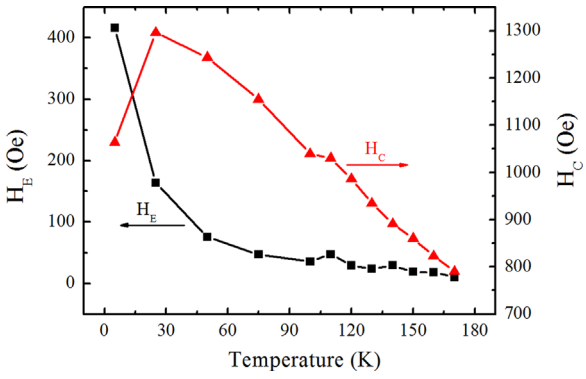

Fig. 5. (Color online) Temperature dependence of H_E and H_C in a temperature range of 10–170 K.

Typical exchange bias effect is observed at 5 K once the sample is cooled in an external field. We consider that the exchange coupling between AFM interactions at APBs and FM spins in the neighboring Fe_3O_4 domains is responsible for the observed EB effect. Training effect is observed in the Fe_3O_4 film: H_E shows a linear relation with $1/n^{1/2}$, and H_C dropped with the measurement cycles. As the temperature increased, the reducing H_E and H_C are observed. The EB effect observed in room temperature epitaxial Fe_3O_4(111) film shows good reproducibility, which might have potential application on spintronics.

Acknowledgment

This work was supported by the National Basic Research Program of China (Projects no. 2010CB630704 and 2012CB921403).

References

[1] W.H. Meiklejohn, C.P. Bean, Phys. Rev. 102 (1956) 1413.
[2] J. Nogués, Ivan K. Schuller, J. Magn. Magn. Mater. 192 (1999) 203.
[3] Ch. Binek, S. Polisetty, Xi He, A. Berger, Phys. Rev. Lett. 96 (2006) 067201.
[4] Yan-kun Tang, Young Sun, Zhao-hua Cheng, Phys. Rev. B 73 (2006) 174419.
[5] R.P. Singh, C.V. Tomy, s.K. Grover, Appl. Phys. Lett. 97 (2010) 182505.
[6] Kenji Yoshii, Appl. Phys. Lett. 99 (2011) 142501.
[7] D. Gilks, L. Lari, Z. Cai, O. Cespedes, A. Gerber, S. Thompson, K. Ziemer, V.K. Lazarov, J. Appl. Phys. 113 (2013) 17B107.
[8] S.B. Ogale, K. Ghosh, R.P. Sharma, R.L. Greene, R. Ramesh, T. Venkatesan, Phys. Rev. B 57 (1998) 7823.
[9] J.F. Bobo, D. Basso, E. Snoeck, C. Gatel, D. Hrabovsky, J.L. Gauffier, L. Ressier, R. Mamy, S. Visnovsky, J. Hamrle, J. Teillet, A.R. Fert, Eur. Phys. J. B 24 (2001) 43.
[10] J.-B. Moussy, S. Gota, A. Bataille, M.-J. guittet, M. Gautier-Soyer, F. Delille, B. Dieny, F. Ott, T.D. Doan, P. Warin, P. Bayle-Guillemaud, C. Gatel, E. Snoeck, Phys. Rev. B 70 (2004) 174448.
[11] G. Hu, Y. Suzuki, Phys. Rev. Lett. 89 (2002) 276601.
[12] D.T. Margulies, F.T. Parker, M.L. Rudee, F.E. Spadas, J.N. Chapman, P.R. Aitchison, A.E. Berkowitz, Phys. Rev. Lett. 79 (1997) 5162.
[13] Xiangbo Liu, Huibin Lu, Meng He, Le Wang, Hongfei Shi, Kuijuan Jin, Can Wang, Guozhen Yang, J. Phys. D: Appl. Phys. 47 (2014) 105004.
[14] W. Eerenstein, T.T.M. Palstra, T. Hibma, S. Celotto, Phys. Rev. B 66 (2002) 201101(R).
[15] R.G.S. Sofin, Han-Chun Wu, I.V. Shvets, Phys. Rev. B 84 (2011) 212403.
[16] W. Eerenstein, T.T.M. Palstra, S.S. Saxena, T. Hibma, Phys. Rev. Lett. 88 (2002) 247204.
[17] A. Hochstrat, Ch. Binek, W. Kleemann, Phys. Rev. B 66 (2002) 092409.